

Supporting Information

Synthesis of rod-shaped gold nanorattles with improved plasmon sensitivity and catalytic activity

Yuriy Khalavka, Jan Becker and Carsten Sönnichsen*

*Physical Chemistry, Johannes Gutenberg University of Mainz,
Jakob Welder Weg 11, Mainz, 55128, Germany*

* soennichsen@uni-mainz.de

List of figures:

	Page
Representative TEM images and histograms of a size distribution for the initial silver coated gold nanorods (S1)	S2
Optical spectra of gold rods, silver-coated gold rods, and gold nanorattles (S2)	S3
TEM images of nanorattles grown at room temperature (S3)	S3
TEM image of the nanorattles made of thin-silver layer coated rods (S4)	S4
A typical plasmon shift induced by changing the solvents refractive index (S5)	S4
Dependence of figures of merit (FOM) from the Plasmon resonance wavelength (a) and cumulative probability distribution of the figure of merit derived from measuring single particle spectra (b) (S6)	S5
Stability of the particles (S7)	S6
Estimation of the increasing of surface area in nanorattles compare to nanorods (S8)	S6
TEM images of Pd-rattles with gold core (S9)	S7
Concentration dependence of catalytic activity of gold nanorods and nanorattles (S10)	S7

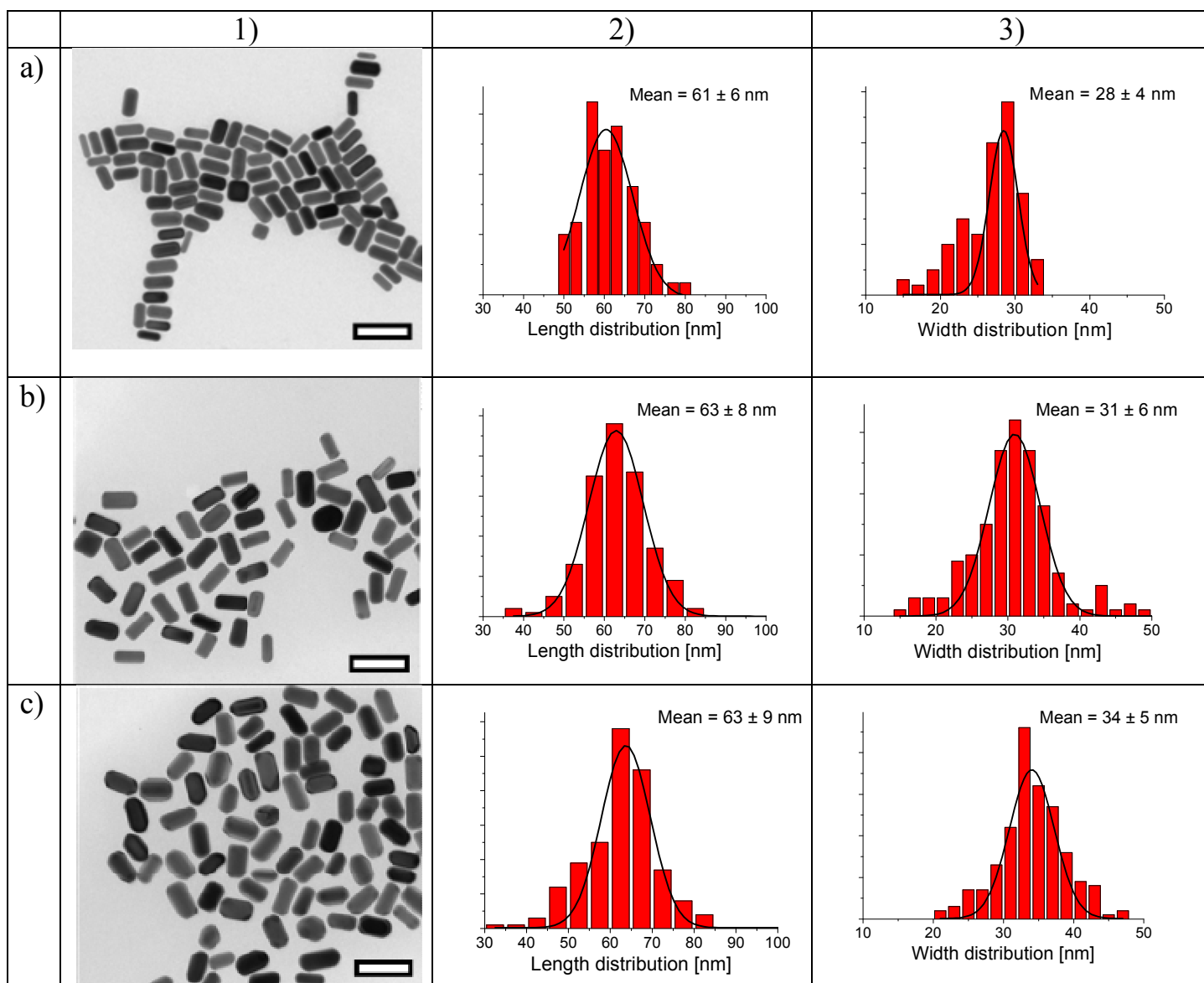


Figure S1. Initial gold nanorods (a) and silver-coated rods used as a template for the cage growth (b, c). TEM images of the samples are shown in column (1). Columns (2) and (3) show histograms for length and width distributions determined from 160 particles, respectively. The thickness of the silver layer deposited onto the gold rods can be estimated from an increase in width: 3 nm for the thin coated rods in row (b) and 6 nm for the thick coated rods in row (c). Scalebars are 100 nm.

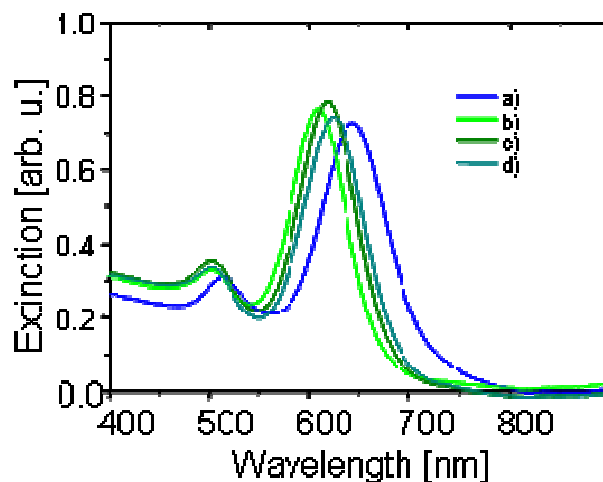


Figure S2. Extinction spectra of the rods (a), the rods coated with thin Ag shell (b) and the rattles (closed (c) and porous (d)) made of them. While the silver coating leads to a blue shift of the resonance wavelength, the replacement of the silver shell with a gold cage shifts the resonance wavelength to the red.

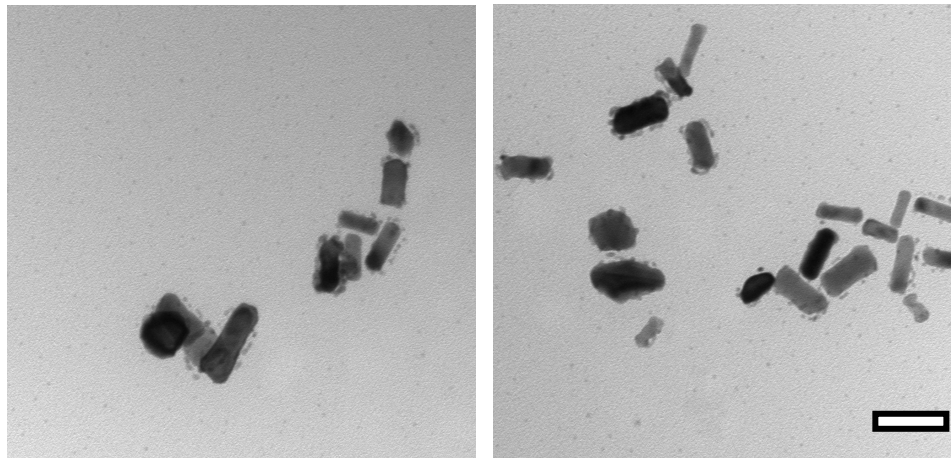


Figure S3. Nanorattles grown at room temperature. Cages around the rods are non-uniform, often directly on the surface of rods, and sometimes residuals of a silver layer are observable. Scalebar is 50 nm.

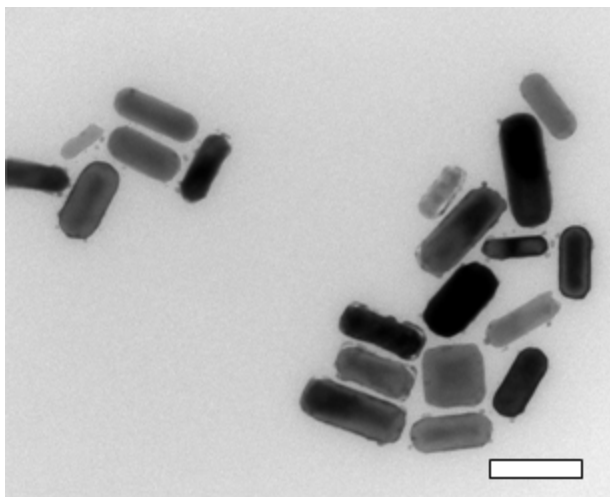


Figure S4. TEM image of the nanorattles made up of thin-silver layer (3 nm) coated rods (scalebar is 50 nm). Only a few rattles show continuous gold shell in comparison to the rattles grown with a 6 nm shell (see Figure 1 in the main text).

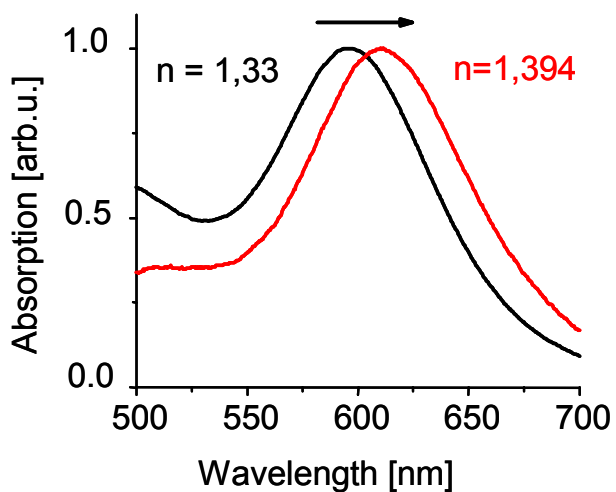


Figure S5. Plasmon shift of the longitudinal peak of nanorattles by changing the surrounding refractive index.

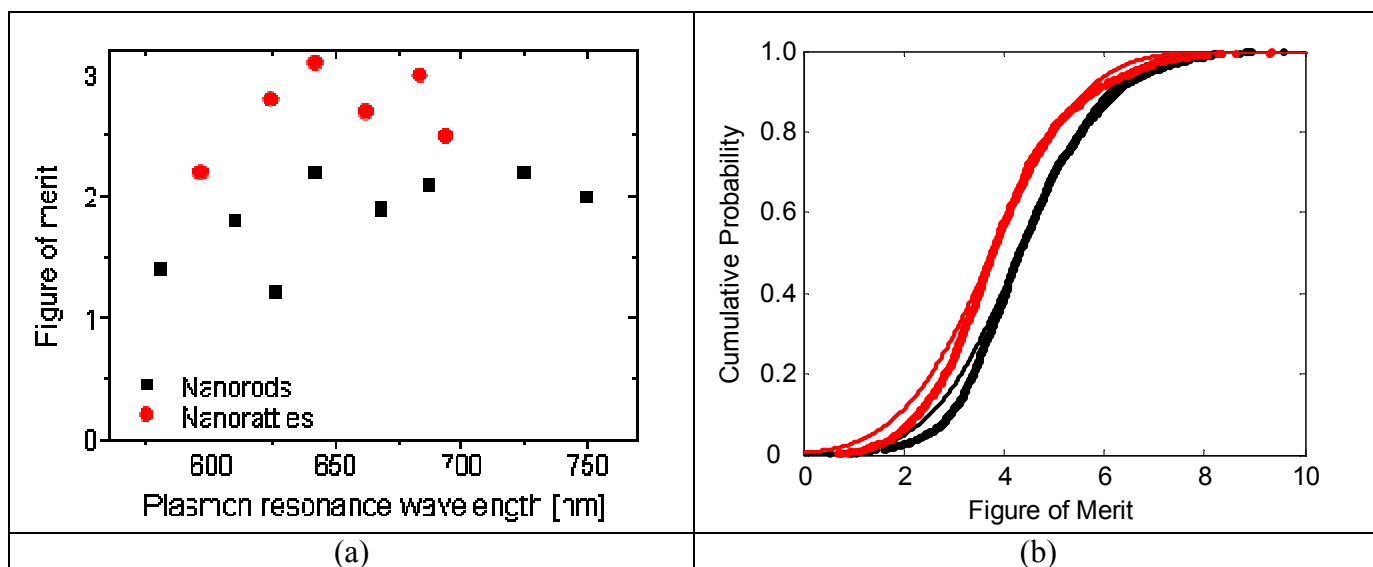


Figure S6. (a) Dependence of the figures of merit (FOM) from the plasmon resonance wavelength for the solutions of gold nanorods and rattles as indicated. (b) Cumulative probability distribution of the figure of merit derived from measuring single particle spectra of 1567 nanorods and 803 nanorattles. The median value is $\text{FOM} = 4.3 \pm 1.4$ and $\text{FOM} = 3.8 \pm 1.5$ for the rods (black) and cages (red), respectively. Although the rattles have a higher Q value compared to the rods (see Fig. 3), they show a smaller FOM value due to the larger FWHM as a result of the stronger plasmon damping in rattles, which increases the FWHM. .

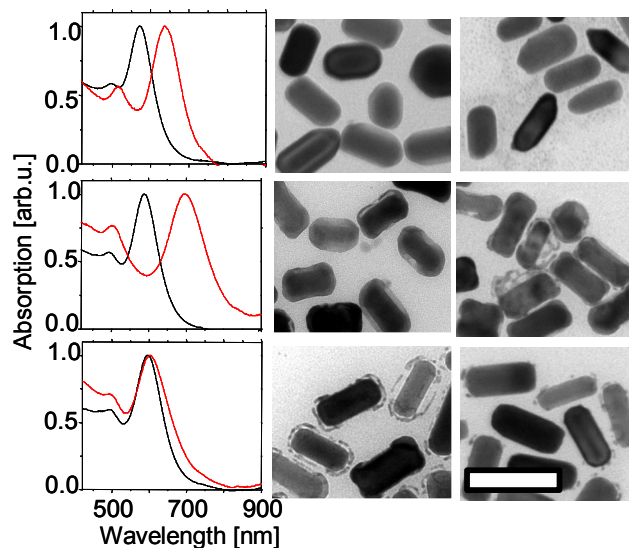


Figure S7. Stability of silver-coated particles, closed and porous nanorattles in aqueous media. Spectra (left column) and TEM images of freshly prepared (middle) and aged particles (right). Black graphs - the freshly prepared particles and red – particles after aging for 21 days. Silver coated rods (upper row), nanorattles with closed outer shell (middle row), and the porous gold nanorattles (bottom row). It is clear that porous nanorattles maintain their resonance wavelength better than closed ones and silver coated rods. Scalebar is 50 nm.

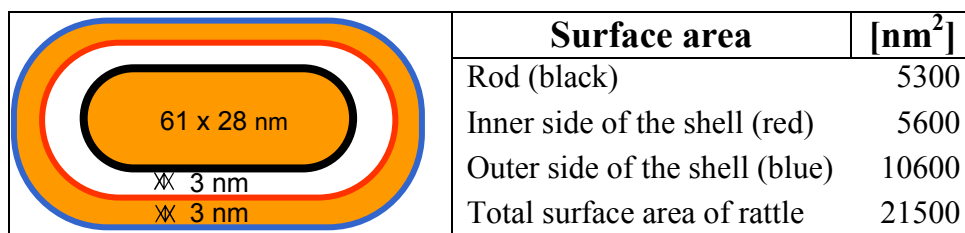


Figure S8. Estimation of the increase of surface area in nanorattles compared to nanorods. Dimensions of the rattle used for the calculations are shown. Total surface area of the nanorattle (21500 nm²) is approximately 4 times bigger than that of the initial rod (5300 nm²).

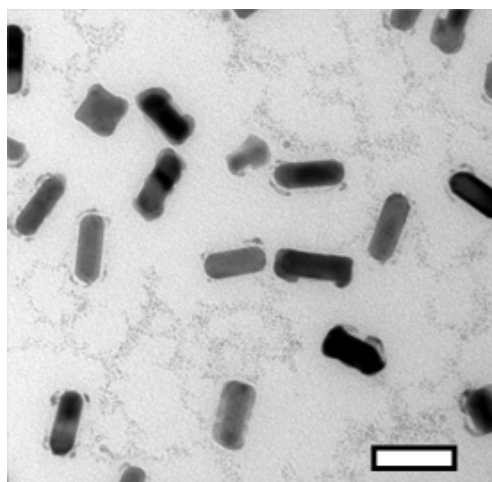


Figure S9. TEM image of the Pd-rattles with gold core used for the catalytic activity measurements. Scalebar is 60 nm.

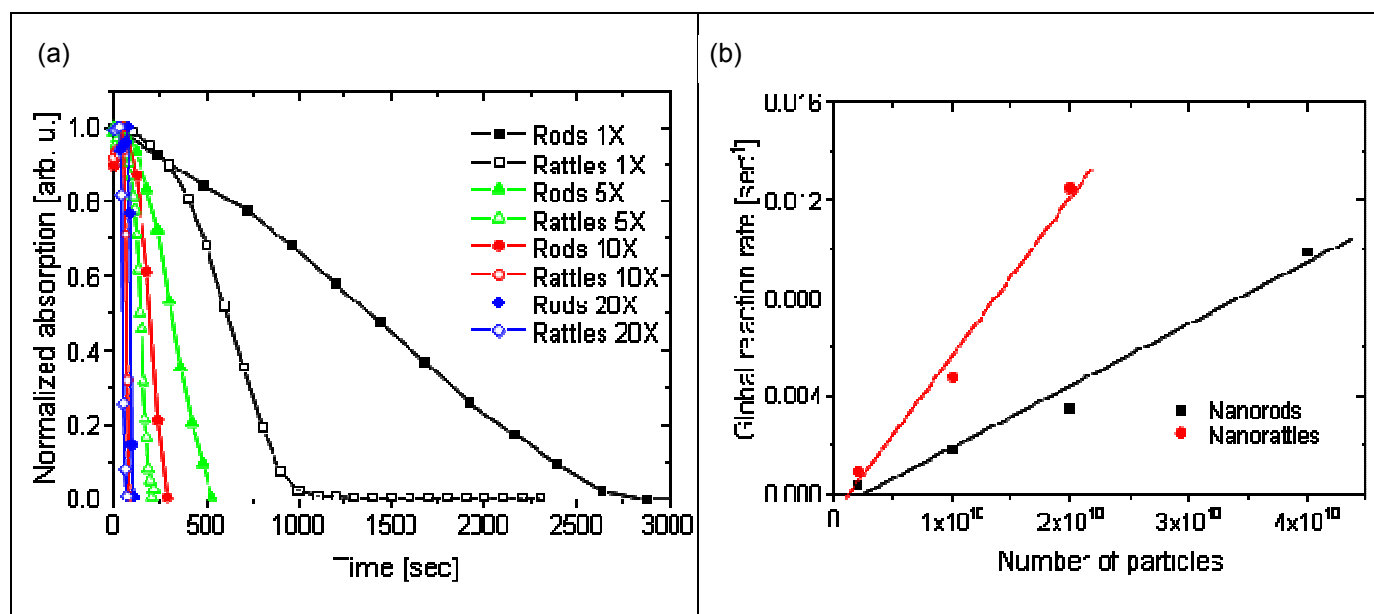


Figure S10. (a) Normalized absorption at the peak position of para-nitrophenol- NaBH_4 as a function of time after adding different amounts of catalyst. Number of particles shown here as 1X is approx. $2 \cdot 10^9$. Z-shape of kinetic curve caused likely by the consecutive nature of this reaction: first sodium borohydride is decomposed on the surface of nanoparticles producing H-atoms, which then react with p-nitrophenol-molecules. (b) Dependence of catalytic activity of gold nanorods and nanorattles on the number of particles added to the reaction mixture. Lines are linear fits. The increase of the reaction rate is in good agreement with an Eley-Rideal mechanism for heterogeneous reactions. This mechanism proposes that only one of the reactants (in our case H-atoms) adsorbs on the surface of the catalyst, and the global reaction rate depends linearly on the total number of active sites or particle concentration.